JOURNAL OF MATERIALS SCIENCE 29 (1994) 157–163

# Mechanical selection of foams and honeycombs used for packaging and energy absorption

J. ZHANG
*Department of Materials Science and Engineering, Case Western Reserve University, Cleveland, OH 44106, USA*

M. F. ASHBY
*Cambridge University Engineering Department, Trumpington St., Cambridge, CB2 1PZ, UK*

The volume of foams used in packaging is enormous. Proper design requires identification of the correct material and selection of the correct density for each particular application. The vast amount of data in the literature is in need of a systematic analysis and a compact presentation. In this paper, the energy-absorption data of each class of cellular materials (such as open-cell elastic foams) are normalized and presented in a single diagram. Diagrams of this type are termed packaging-selection diagrams, and the optimal density of a cellular material can be obtained from them once the maximum permitted stress of the packaging is known. This new approach offers greater generality and simplicity than existing methods, such as the Janssen factor or energy-absorption diagrams.

## 1. Introduction

We live in a world full of packaging. Most commodities are packaged, from food to missiles. Foams and honeycombs are commonly used in packaging. The essence of packaging is the ability to absorb energy but to still keep the peak force on the packaged object below the limit which will cause damage or injury. Cellular materials (such as foams) are especially good at this. Their energy-absorption capacity is compared to that of the equivalent solid in Fig. 1a (after Gibson and Ashby, [1]); for a given energy absorption, the cellular material often generates a lower peak force than the solid. The energy absorbed by the foam per unit volume at the strain $\varepsilon$ is simply the area under the stress–strain curve up to $\varepsilon$ (shown as shaded area in Fig. 1a). As Fig. 1 shows, it is the long plateau in the stress–strain curve (arising from cell collapse due to elastic buckling, plastic yielding or brittle crushing) which allows large energy absorption at a near-constant load.

To absorb energy at a near-constant load, the correct cell-wall material and relative density must be chosen for the foam. Selecting the cell-wall material is relatively simple. Consideration must be given as to whether the packaging material carries a static or repeated loading or whether it is subjected to severe environmental conditions such as high temperatures. An elastomeric cell-wall material is needed for packaging which will be subjected to repeated loading. If the protection is needed only once, a plastic or brittle material is better because such cellular materials are more efficient (the details given later). Choosing the correct density for a given package is more difficult and this paper tries to add some understanding to this problem. If the density is too low, the cells will be crushed before sufficient energy has been absorbed. If the density is too high, the stress will exceed the critical value before sufficient energy can be absorbed. This is best explained by Fig. 1b (taken from [1]), which compares the performance of foams with three different densities.

Four main ways of characterizing the energy absorption of cellular materials have been proposed. These are the Janssen Factor, $J$; the cushion factor, $C$; the Rusch curve; and the energy absorption diagram. In this paper, all existing methods are reviewed. Then packaging-selection diagrams for elastic foams, plastic foams, elastic honeycombs and plastic honeycombs are presented and compared with experimental data. A comparison is made between the energy-absorbing capacities of foams and honeycombs by plotting their packaging-selection diagrams on the same graph. A case study is provided to demonstrate the application of the packaging-selection diagrams to a car-head-rest design.

## 2. Literature review

There is considerable literature on the use of foams for cushioning and packaging. The interested reader might wish to consult the books [1–3], the series of papers by Lockett, Cousins and Dawson [4–6], and the papers by Green *et al.* [7], Rusch [8, 9], Lee and Williams [10], Melvin and Roberts [11], Schwaber and co-workers [12–15] and Maiti *et al.* [16]. The approaches of these authors are summarized in the following paragraphs.

### 2.1. The Janssen factor, $J$

According to Woolam [17], the efficiency of

0022–2461 

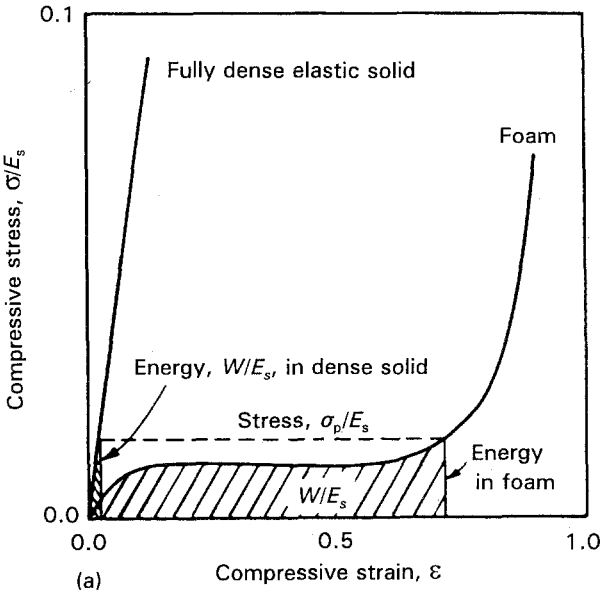


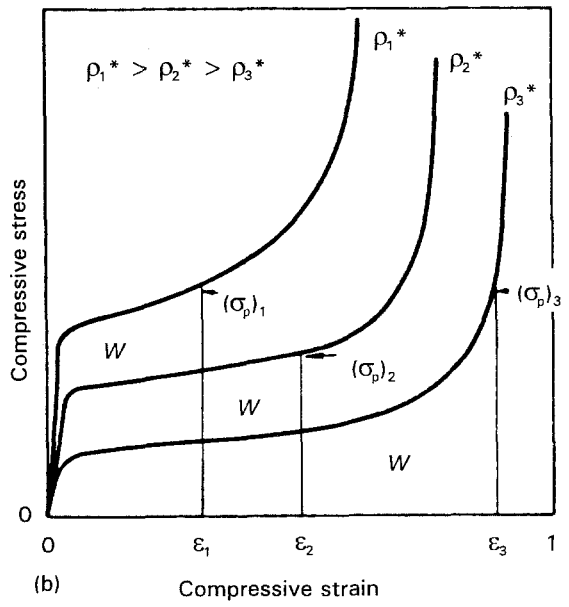


*Figure 1* (a) Stress–strain curves for an elastic solid and a foam made from the same solid, showing the energy per unit volume absorbed at a peak stress, $\sigma_p$. (b) The peak stresses generated in foams of three densities in absorbing the same energy, $W$, are given by $(\sigma_p)_1$, $(\sigma_p)_2$ and $(\sigma_p)_3$. The lowest-density foam bottoms out before absorbing the energy $W$, generating a high peak stress. The highest-density foam also generates a peak stress before absorbing the energy $W$. Between these two extremes, there exists an optimal density, where the energy $W$, is absorbed at the lowest peak stress, (after [1])

a cushioning material in absorbing an energy $J$ can be defined as the ratio of the maximum acceleration experienced by the material, $a_m$, to the acceleration which would be experienced by an ideal absorber, $a_i$

$$J = \frac{a_m}{a_i} \tag{1}$$

This "ideal" absorber can absorb energy at a constant force, $F$, and it can deform completely, so its acceleration is

$$a_i = \frac{F}{m} = \frac{mv^2}{2hm} = \frac{v^2}{2h} \tag{2}$$

where $v$ and $m$ are the initial speed and the mass of the cushioned object, respectively, and $h$ is the height of the cushioning material. The Janssen factor, $J$, is often plotted against the impact energy, $W$, per unit volume of the cushioning material, as shown in Fig. 2a.

## 2.2. The cushion factor, $C$

The cushion factor, $C$, is the ratio of the peak stress developed in the cushion to the energy stored per unit volume of the cushion. Gordon [18] plots this factor against the peak stress by using data on the uniaxial stress–strain behaviour of foams (Fig. 2b). One point is worth noting: the factor is equivalent to the Janssen factor, $J$, in dynamic testing (such as drop-weight testing)

$$C = \frac{\sigma_p}{W} = \frac{(ma_m/A)}{(mv^2/2Ah)} = J \tag{3}$$

where $A$ is the area of the cushion.

## 2.3. The Rusch curve

Rusch [8, 9] notes that the shape of the stress–strain curve can be defined by an empirical shape factor, $\psi(\varepsilon)$, in the form

$$\sigma = E_f \varepsilon \psi(\varepsilon) \tag{4}$$

where $\sigma$ is the compressive stress, $\varepsilon$ is the strain, and $E_f$ is the Young's modulus of the foam. Rusch further defines $K$, the energy-absorbing efficiency, as the maximum deceleration of a material packaged by an ideal material to that packaged by the foam under investigation, $d_m$:

$$K = \frac{v^2}{2hd_m} = \frac{1}{J} \tag{5}$$

Another dimensionless quantity, $I$, is defined as the impact energy per unit volume of foam divided by $E_f$. The optimum foam for energy absorption for a given peak stress can be found by plotting $I/K$ against $I$ (Fig. 2c).

## 2.4. Energy-absorption diagrams

Maiti *et al.* [16] have further improved the Rusch method. The peak stress and energy per unit volume (Fig. 2d) are normalized by the Young's modulus of the solid, $E_s$, which is more general than the Rusch method. However, it is rather difficult to decide the exact point at which the envelope touches the individual curves, as these curves tend to have broad shoulders. As a result, the optimal density may not be readable with good precision.

In this paper, a more direct approach is introduced – the packaging-selection diagram, which allows determination of the optimal density and the energy absorbed, once the maximum permitted stress is known. These diagrams can also incorporate dynamic results. This method may complement and avoid some of the practical difficulties in the existing methods.

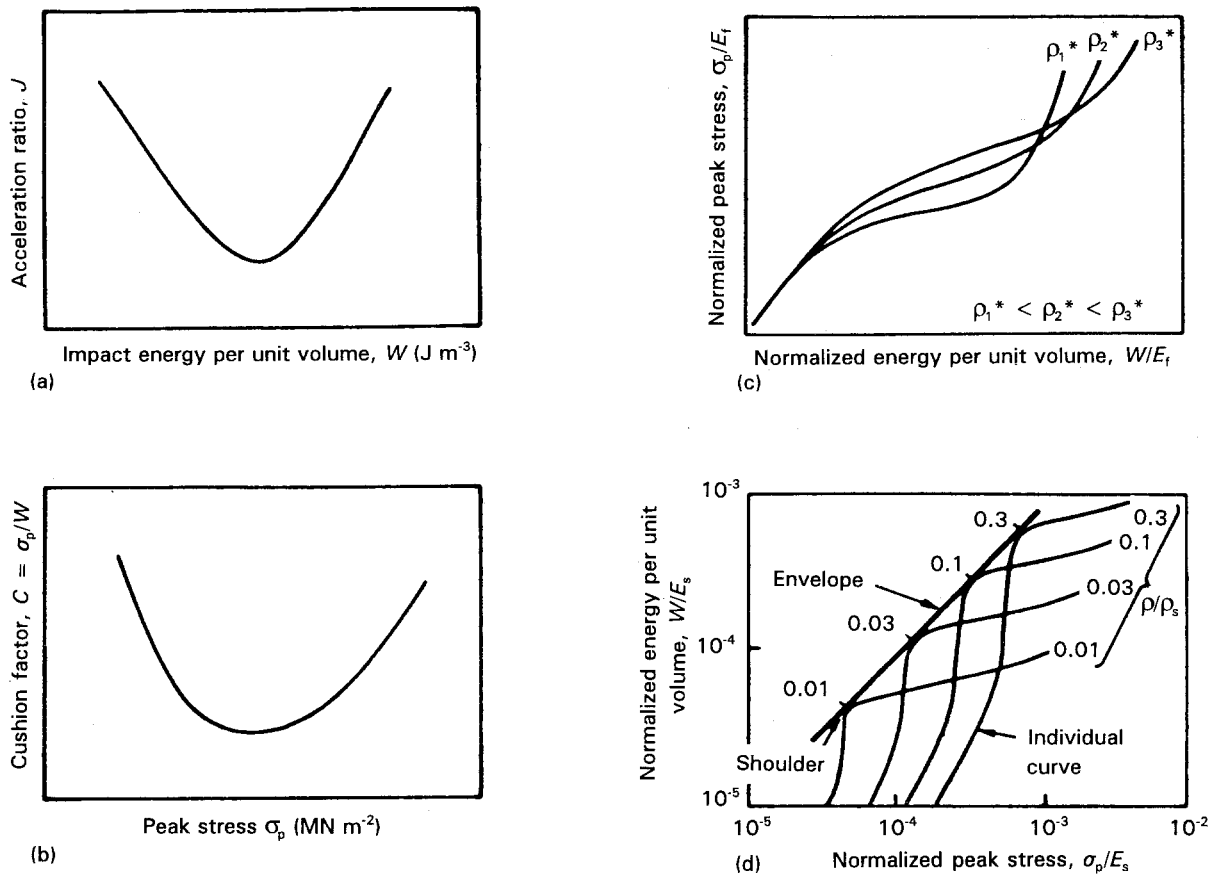


*Figure 2* Four diagrams which are used to characterize energy absorption: (a) the Janssen factor, $J$; (b) the cushion factor, $C$; (c) the Rusch curve; and (d) the energy-absorption diagram.

## 3. Normalization of stress–strain behaviour

An open-cell foam can be modelled as an array of polyhedral cells. A representative unit cell is assumed to be made of beams with equal lengths $l$, and cross-sections, $t^2$. The foam is considered to be an aggregate of these representative units. The force, $P$, acting on each of these beams [1] can be related to the global stress on the foam:

$$P \propto \sigma l^2 \tag{6}$$

First consider the post-collapse behaviour of flexible foams under uniaxial compression. Looking at a typical beam AB (shown in Fig. 3), its curvature, $d\theta/ds$, is given by

$$E_s I \frac{d\theta}{ds} = -M \propto Pl \propto \sigma l^3 \tag{7}$$

where $E_sI$ represents the flexural rigidity of the beam in the plane of bending; $\theta$ is the angle between the tangent to the cell edge and the $x$-axis; and $s$ is measured along the edge.

If the stress is normalized by the initial collapse stress of the foam ($\sigma^* \propto E_s I/l^4$, see [1]) and the dimensionless length $\bar{s}$ is used, (that is, $\sigma/\sigma^* = \bar{\sigma}$ and $s/l = \bar{s}$), the above equation becomes:

$$\frac{d\theta}{d\bar{s}} \propto \frac{\sigma}{\sigma^*} = \bar{\sigma} \tag{8}$$

Although each cell within a foam sample can be geometrically different, foams with varying density

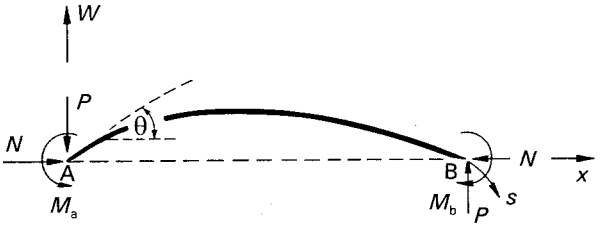


*Figure 3* A diagram used for the analysis of bending deformation in a beam.

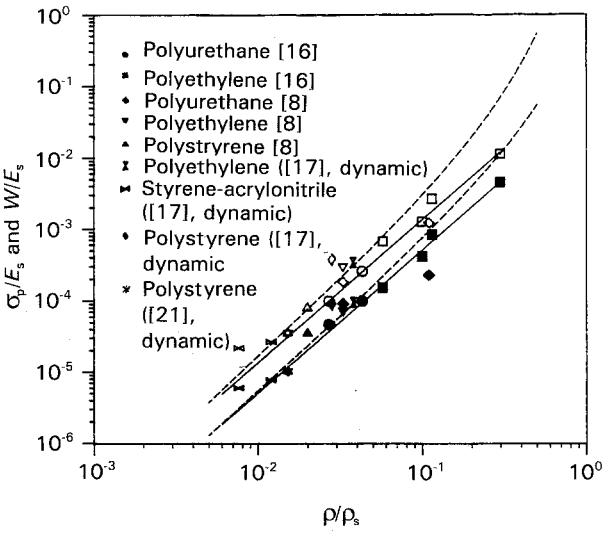


*Figure 4* The packaging-selection diagram for elastic foams. Both the theoretical lines and the experimental data appear in pairs, with the stress lying above the energy absorbed. A peak stress is plotted as an open symbol while the corresponding energy absorbed is shown by the same symbol but shaded: (—) primary theory, and (– – –) refinement.

and cell sizes are visualized as being related to each other by a simple geometrical scaling. Under the normalized stress, $\bar{\sigma}$, all the corresponding positions in the frameworks of foams of varying densities and materials which have the same $\bar{s}$ will have the same angle or the same deformed geometrical shape. As a result, the same amount of post-collapse stress, $\bar{\sigma}$, is related to the same strain, $\varepsilon$. A single stress–strain curve would give a good description for all flexible foams.

Similarly, the stress–strain curves of flexible honeycombs under uniaxial compression can be expressed by a single function if the same normalization procedure is followed. In the case of plastic foams or plastic honeycombs, the upper bounds and lower bounds of the stress–strain curves can be normalized in a similar way to give a single curve for each of them. Therefore, the true stress–strain behaviour of plastic foams or honeycombs can be approximated by a single curve in a dimensionless stress–strain space.

The cell corners in foam structures contribute little to the deformation. As a result, foams with higher relative density tend to density at a lower strain (Fig. 1b). A refinement [19] can be obtained by incorporating these corners (or the "dead volume") or, similarly, the densification strain into consideration. In the refined model, the stress and the strain are normalized by the initial collapse stress and the densification strain, respectively, to give a single stress–strain curve describing one class of cellular materials.

## 4. Optimal selection of foams and honeycombs as energy absorbers

In packaging, the aim is to absorb as much of the energy of the packaged object as possible while at the same time keeping the force on the object below the limit which will cause damage. In mathematical terms, a maximum in the absorbed energy is sought, subject to a given constraint on the stress:

$$\left.\begin{aligned} W &= \int \sigma \, d\varepsilon = \int_0^{\varepsilon} f(\rho^*)\, k(\varepsilon)\, d\varepsilon = f(\rho^*)\, k_1(\varepsilon) \\ \sigma &= f(\rho^*)\, k(\varepsilon) = \sigma_p \end{aligned}\right\} \quad (9)$$

where $\rho^*$ is the relative density – the ratio of the density of the foam, $\rho$, to that of the base solid, $\rho_s$; $k(\varepsilon)$ is the shape function of the stress–strain curve; $k_1(\varepsilon)$ is the integral of $k(\varepsilon)$ over strain; $f(\rho^*)$ is the initial collapse stress, $\sigma^*$; and $\sigma_p$ is the maximum permitted stress set by a given application.

A Lagrange function is constructed as follows:

$$\begin{aligned} L(\rho^*, \varepsilon, \lambda) &= W + \lambda(\sigma - \sigma_p) \\ &= f(\rho^*) k_1(\varepsilon) + \lambda[f(\rho^*)\, k(\varepsilon) - \sigma_p] \end{aligned} \quad (10)$$

The partial derivatives of the constructed function must all be zero when the conditional maximum is reached, leading to:

$$k_1(\varepsilon)\, k'(\varepsilon) = k^2(\varepsilon) \quad (11)$$

From this equation, the strain $\varepsilon_m$, at which the maximum $W$ is reached, can be obtained once the shape function, $k(\varepsilon)$, is known. Then the optimal density and the energy absorbed can be obtained by substituting $\varepsilon_m$ into Equation 9. The energy absorbed per unit volume can be expressed as:

$$W = C_1 \sigma_p \quad (12)$$

where $C_1$ is a constant representing the energy-absorbing efficiency.

The initial part of the stress–strain curve before collapse is not considered here, since it makes little contribution to the total energy absorbed. The approximate shape functions for various types of isotropic foams and honeycombs of regular hexagonal cells are obtained from experimental stress–strain curves (see [19] for details). Solutions of the optimal density and the maximum amount of energy absorbed under the permitted stress for these materials are provided in Table I.

A large amount of data from both static and dynamic tests are available for the optimal packaging design. They are presented in U-shaped curves in the case of the Janssen factor or the cushion factor. These plots contribute to the understanding of maximizing the energy absorption under a given critical stress. However, to design engineers, the optimal points are

TABLE I The optimal selection of EF (elastic foams), PF (plastic foams), EH (elastic honeycombs) and PH (plastic honeycombs) as energy absorbers

| Type | Shape function, $k(\varepsilon)$ ([19]) | Initial collapse stress, $f(\rho^*)$ | Optimal density, $\rho^*$ | Energy $W/\sigma_p = C_1$ |
|---|---|---|---|---|
| EF | $0.95/(1-\varepsilon)$ | $0.05E_s(\rho^*)^2$ ([1]) | $2.77(\sigma_p/E_s)^{1/2}$ | 0.38 |
| PF | $1 \quad \varepsilon \leqslant 0.5$<br>$5 - [16 - 100(\varepsilon - 0.5)^2]^{0.5} \quad \varepsilon > 0.5$ | $0.32\sigma_{ys}(\rho^*)^{3/2}$ ([19]) | $2.03(\sigma_p/\sigma_{ys})^{2/3}$ | 0.50 |
| Out-of-plane EH | $1 \quad \varepsilon \leqslant 0.5$<br>$\infty \quad \varepsilon > 0.5$ | $7.2E_s(\rho^*)^3$ ([22]) | $0.52(\sigma_p/E_s)^{1/3}$ | 0.50 |
| In-plane EH | $1 \quad \varepsilon \leqslant 0.5$<br>$\infty \quad \varepsilon > 0.5$ | $0.14E_s(\rho^*)^3$ ([1]) | $1.93(\sigma_p/E_s)^{1/3}$ | 0.50 |
| Out-of-plane PH | $1 \quad \varepsilon \leqslant 0.75$<br>$\infty \quad \varepsilon > 0.75$ | $3.2\sigma_{ys}(\rho^*)^{5/3}$ ([19]) | $0.50(\sigma_p/\sigma_{ys})^{3/5}$ | 0.75 |
| In-plane PH | $1 \quad \varepsilon \leqslant 0.5$<br>$\infty \quad \varepsilon > 0.5$ | $0.28\sigma_{ys}(\rho^*)^2$ ([19]) | $1.89(\sigma_p/\sigma_{ys})^{1/2}$ | 0.50 |

of most interest. In the case of U-shaped curves, this is the lowest point, while in the case of energy-absorption diagrams and Rusch's curves it is the point which touches the envelope. We replot these optimal points in our package-selection diagrams and compare them with our theoretical modelling. One thing is worth noting: each stress or energy value in the following plots is normalized against the solid properties $\rho_s$, $E_s$ and $\sigma_{ys}$ measured at the strain-rate and the temperature at which the test was performed. The normalizing properties $\rho_s$, $E_s$ and $\sigma_{ys}$ for low strain-rates at room temperature are given in Table II. A typical dynamic test at the strain rate around 50/s will increase the solid Young's modulus $E_s$, and yield strength, $\sigma_{ys}$, by a factor of around 2.5. As a result of this normalization, curves of the data for the same foams tested at different strain-rates or drop heights lie on top of each other.

The data and the predictions for elastic foams are plotted in Fig. 4. The agreement for the low relative-density range is good. There are more discrepancies when the density becomes larger. The data and the predictions for plastic foams are plotted in Fig. 5. The agreement is good for both the low and the high relative-density ranges.

There is considerable discrepancy in the measurements of solid properties $\sigma_{ys}$ and $E_s$. Also, the initial collapse stress of a foam could vary considerably from the theoretical prediction. It is a more realistic design methodology to identify a few possible cell-wall materials and their corresponding optimal densities from the packaging-selection diagrams and then to conduct simple compression tests to measure their initial collapse stresses. As calculated in Table I, the best plastic foams will be those that have initial collapse stresses around 93% of the critical stress, $\sigma_p$, whereas the best elastic foams will be those with initial stresses around 38% of $\sigma_p$.

The book by Mustin [2] contains a large amount of data of honeycombs under both static and dynamic loading. In principle, this data could also be plotted and compared with the theoretical predictions. A complication exists because their hexagonal cell angles are not always constant. Although, in general, the stress–strain behaviour and the mechanical properties of the honeycombs [22, 23] are strongly dependent on the density and are rather weakly dependent on the cell angles, the packaging-selection diagrams generated from the experimental data are expected to show more scatter.

The advantage of plastic foams or honeycombs is that, compared with elastic foams or honeycombs, they provide a better energy-absorption capacity under the same critical stress, $\sigma_p$. However, the plastic ones absorb much less energy after the first impact. The elastic ones can absorb energy repeatedly, and their energy-absorption capacity is not reduced appreciably after the first loading. In comparing honeycombs with foams (Figs 6 and 7), when honeycombs are loaded in the out-of-plane direction they are better than their counterparts in their energy absorption. In addition, the optimal density of honeycombs for a given critical stress is generally smaller than that of

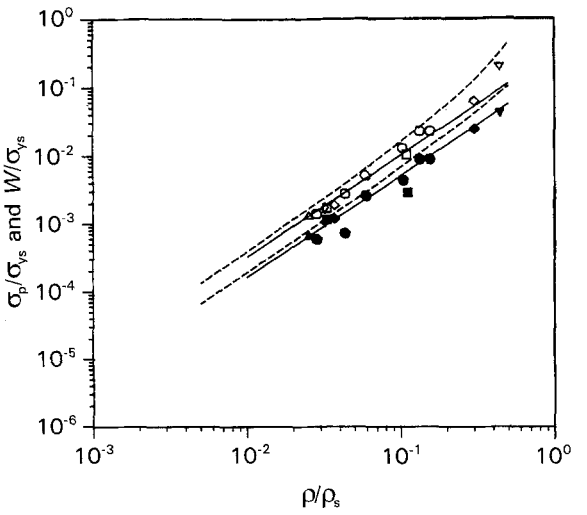


*Figure 5* The packaging-selection diagram for plastic foams. Both the theoretical lines and the experimental data appear in pairs with the stress lying above the energy absorbed. A peak stress is plotted as an open symbol while the corresponding energy absorbed is shown by the same symbol but shaded: (—) primary theory, (– – –) refinement, (○) polymethylacrylamid [16], (■) polyurethane ([8], – 196 °C), (○) polyurethane [8], (▼) ABS [8], (▲) polyurethane ([17], dynamic), and (◆) phenolic [8].

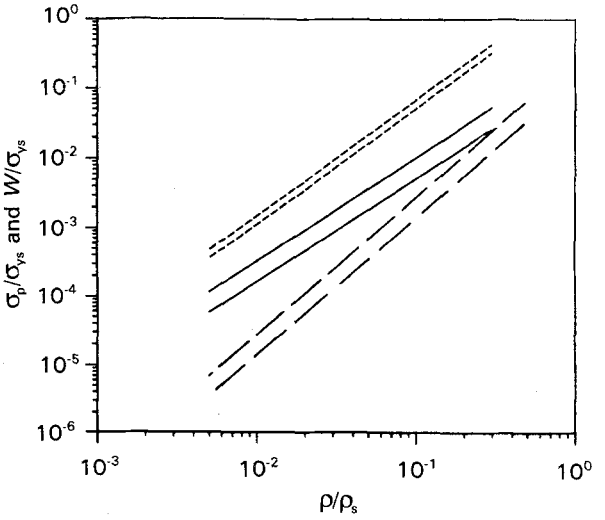


*Figure 6* The packaging-selection diagrams for (—) plastic foams, (– – –) plastic honeycombs (out-of-plane), and (· · ·) plastic honeycombs (in-plane). Plastic honeycombs loaded out-of-plane had a better energy-absorption capacity than plastic foams. For a given application, the optimal honeycomb is much lighter than its foam counterpart.

TABLE II cell-wall properties

| Materials | $\rho_s$(Mg m$^3$) | $E_s$(GN m$^{-2}$) | $\sigma_{ys}$(MN m$^{-2}$) |
|---|---|---|---|
| ABS [20] | 1.07 | 2.6 | 70 |
| Phenolic [20] | 1.28 | 0.038 | 100 |
| Polyethylene [1] | 0.92 | 0.2 | – |
| Polymethacrylimid [16] | 1.2 | 3.6 | 360 |
| Polyurethane, rigid [1] | 1.2 | 1.6 | 127 |
| Polyurethane, flexible [1] | 1.2 | 0.045 | – |
| Polystyrene, flexible [20] | 1.05 | 3.0 | 80 |
| Styrene-acrylonitrile [20] | 1.05 | 3.0 | 80 |

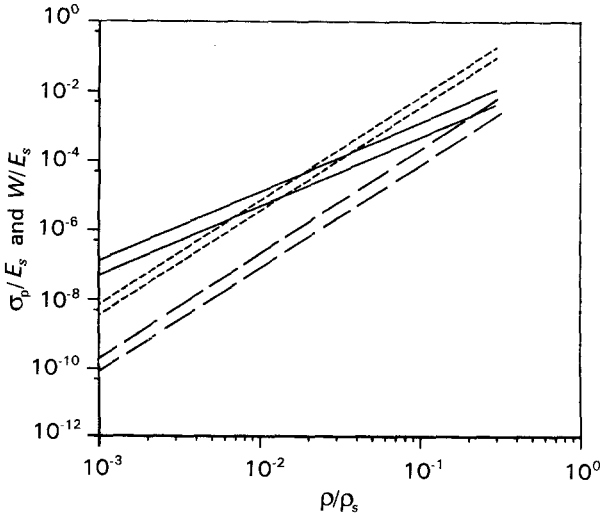


*Figure 7* The packaging-selection diagrams for (—) elastic foams (– – –) plastic honeycombs, (out-of-plane), and (· · ·) elastic honeycombs (in-plane). Elastic honeycombs loaded out-of-plane had a better energy-absorption capacity than elastic foams. For a given application, the optimal honeycomb is much lighter than its foam counterpart.

foams, which makes them very attractive when weight savings are crucial. On the other hand, honeycombs loaded in the in-plane directions are inferior to foams in their weight savings.

## 5. A case study on car-head-rest design

Many packaging theories have been proposed to date. As reviewed earlier, these theories either do not directly provide the optimal density or they have some practical difficulties in giving the density. A large amount of experimental data on foams has also been generated. Companies like Dow Chemical use "cushion" curves [24] in designing package components. These cushion curves are material specific as well as component-geometry specific. Understandably, the amount of experimental work involved is considerable. Organizing this data into a readable database is also difficult. The packaging-selection diagrams proposed in this paper provide a direct and systematic approach to the selection of foams for a given impact or in static situations. Their advantage over other methods is that they bring together foam-material types and strain-rate variables in one diagram. From these diagrams, the optimal density and the energy absorbed can be read out with ease and with adequate precision. To illustrate this, a car-head-rest design is studied.

According to Gibson and Ashby [1], the head-rest padding of a contemporary family car is made of a flexible polyester foam with a relative density close to 0.06. The other design constraints provided by Gibson and Ashby [1] are as follows: the maximum permissible deceleration $a = 50$ g, the area of contact between a head and the rest is $A = 0.01\ m^2$, the mass of a head $m = 2.5$ kg, the thickness of the padding is $t = 0.17$ m.

The maximum permissible stress is given by:

$$\sigma_p = ma/A = 1.23 \times 10^5\ N\,m^{-2}$$

The static Young's modulus of solid polyester is $15\ MN\,m^{-2}$. Assuming that the dynamic modulus $E_s$ (when the car slows down from a speed of a few miles per hour, the expected strain rate of the head-rest padding is around $100/s$. This value of the strain rate will typically give a dynamic modulus which is about 2.5 times the static modulus) is $37.5\ MN\,m^{-2}$, then

$$\sigma_p/E_s = 3.3 \times 10^{-3}$$

Using the prediction from the refined model in Fig. 4, the optimal relative density is 0.1 and the maximum energy absorbed is

$$W = 0.24\,\sigma_p = 30.6\ kJ\,m^{-2}$$

The maximum collision speed at which the foam padding can protect the car occupants is:

$$W = \frac{0.5\,mv^2}{At} = 30.6\ kJ\,m^{-2}$$

leading to

$$v = 6.4\ m\,s^{-1} = 14.3\ m.p.h$$

This protection speed is much higher than the 6 m.p.h. (miles per hour) calculated by Gibson and Ashby [1] for the current head-rest-padding mode of a polyester foam with a relative density of 0.06.

Applying a similar selection procedure to foams made of polyethylene with a dynamic modulus of $500\ MN\,m^{-2}$ yields an optimal density of 0.034 and a protection speed of 15.9 m.p.h. In this case, the energy absorption efficiency, $C_1$, is 30%. As seen from Fig. 4, the efficiency can be improved up to 38% by choosing more rigid foams made of materials with a higher Young's modulus. The optimal densities for more rigid foams are lower as well. As a result, weight savings and the energy efficiencies can be achieved at the same time when a flexible foam made of a stronger solid material is utilized. Designing a packaging is a complex issue. Cost, appearance and other design considerations [25] need to be weighed, and a final choice made and tested.

Can another type of cellular material be chosen to make head-rest paddings even lighter and more energy-absorption efficient? Nomex-paper honeycombs might be a potential choice. As can be seen from Table I, by choosing flexible honeycombs (loaded in the out-of-plane direction), the efficiency, $C_1$, can be increased to about 50%. The dynamic Young's modulus of Nomex paper is about 2.2 GPa. Using the data for elastic honeycombs from Table I, the optimal relative density can be calculated as having a value of about 0.01. The protection speed is increased to 20.5 m.p.h. In this case, the total weight saving in using Nomex honeycombs rather than polyester foams is as high as 90%.

## 6. Conclusions

The energy-absorption diagrams of the type proposed

in this paper are not limited to foams and honeycombs. Similar diagrams can be developed for other classes of materials if their stress–strain curves have a similar shape. Density is always an important parameter both in terms of its effect on the stress–strain behaviour and the weight-saving considerations pertinent to many engineering applications. A general approach exists where the permissible stress is normalized by a solid property, and is then plotted against the relative density. The solid property chosen should be the property affecting the initial collapse stress the most. This is reminiscent of the approach to materials selection pioneered by Ashby [26], where all the materials properties are mapped against density. Even if a constitution law governing the collapse stress with regard to the relative density may not exist, empirical energy diagrams like those in Figs 4 and 5 can be developed, and empirical design criteria like those in Table I can then be extracted. The optimal density and the maximum amount of energy absorbed, of course, can be read directly from these diagrams with reasonable precision.

Packaging systems employing cellular materials are traditionally designed with an experimental database, requiring a large number of impacts tests [2]. The packaging-selection diagrams in this paper allow empiricism to be combined with physical modelling. If properly used, the number of experiments needed in the design process can be significantly reduced. The diagrams are adequate for the broad comparisons required in conceptual design, and, in most cases, for the rough calculations of embodiment design. They may not be appropriate for detailed design calculations where it may be necessary to conduct a few selected experiments. Packaging-selection diagrams are helpful in narrowing down the range of densities and choices of the solid base materials to be tested.

## References


1. L. J. GIBSON and M. F. ASHBY, "Cellular solids: structure and properties" (Pergamon Press, Oxford, 1988).
2. G. S. MUSTIN, "Theory and practice of cushion design" (US Government Printing Office, Washington, DC, 1968).
3. N. C. HILYARD (editor) "Mechanics of cellular plastics" (Applied Science Publishers, London, 1982).
4. R. R. COUSINS, *J. Appl. Polymer Sci.* **20** (1976) 2893.
5. *Idem.*, "Design guide to the use of foams for crash padding", National Physics Laboratory, NPL Report DMA 237, London (1976).
6. F. J. LOCKETT, R. R. COUSINS and D. DAWSON, *Plast. Rubber Proc. Appl.* **1** (1981) 25.
7. S. J. GREEN, F. L. SCHIERLOH, R. D. PERKINS and S. G. BABCOCK, *Exp. Mech.* March (1969) 103.
8. K. C. RUSCH, *J. Appl. Polymer Sci.* **14** (1970) pp. 1263 and 1433.
9. *Idem., J. Cell. Plast.* **7** (1971) 78.
10. W. M. LEE and B. M. WILLIAMS, *ibid.* **7** (1971) 72.
11. J. W. MELVIN and V. L. ROBERTS, *ibid.* **7** (1971) 97.
12. E. A. MEINECKE and D. M. SCHWABER, *J. Appl. Polymer Sci.* **14** (1970) 2239.
13. E. A. MEINECKE, D. M. SCHWABER and R. R. CHIANG, *J. Elastoplast.* **3** (1971) 19.
14. D. M. SCHWABER and E. A. MEINECKE, *J. Appl. Polymer Sci.* **157** (1971) 2381.
15. D. M. SCHWABER, *Polymer-Plast. Technol. Engng.* **2** (1973) 231.
16. S. K. MAITI, L. J. GIBSON and M. F. ASHBY, *Acta Metal.* **32** (1984) 1963.
17. W. E. WOOLAM, *J. Cell. Plast.* **4** (1968) 79.
18. G. A. GORDON, "Testing and approval, impact strength and energy absorption" (PIRA 1974).
19. J. ZHANG, PhD thesis, Cambridge University Engineering Department, Cambridge, UK (1989).
20. Handbook of industrial materials, 1st Edn, Trade and Technical Press, Surrey, UK.
21. J. DRYSDALE, G. A. GORDON, E. E. WHEELER and P. D. MARSDEN, Package, 34 (396, 399 and 400), (March, June, and July) (Memoir No. 6, Packaging Division, PATRA) (1963).
22. J. ZHANG and M. F. ASHBY, *Int. J. Mech. Sci.* **34** (1992) 475.
23. *Idem., ibid.* **34** (1992) 491.
24. Dow Chemical Company A Guide to Protective Package Design, Form No. 172-1150-87 (Dow, Midland, OH, 1987).
25. *Idem.*, Cushioning, Form No. 172-1120-88 (1988).
26. M. F. ASHBY, *Acta Metall.* **37** (1989) 1273.



*Received 3 September*
*and accepted 26 October 1992*